THE ASTROPHYSICAL JOURNAL, 440:697–705, 1995 February 20

THE GALACTIC DISTRIBUTION OF ALIPHATIC HYDROCARBONS IN THE DIFFUSE INTERSTELLAR MEDIUM

SCOTT A. SANDFORD, YVONNE J. PENDLETON, AND LOUIS J. ALLAMANDOLA
NASA/Ames Research Center, Mail Stop 245-6, Moffett Field, CA 94035
Received 1994 May 23; accepted 1994 September 2

ABSTRACT

The infrared absorption feature near 2950 cm^{-1} (3.4 μm), characteristic of dust in the diffuse interstellar medium (ISM), is attributed to C—H stretching vibrations of aliphatic hydrocarbons. We show here that the strength of the band does not scale linearly with visual extinction everywhere, but instead increases more rapidly for objects near the center of the Galaxy, a behavior that parallels that of the Si—O stretching band due to silicate materials in the diffuse ISM. This implies that the grains responsible for the diffuse medium aliphatic C—H and silicate Si—O stretching bands are different from those responsible for much of the observed visual extinction. It also suggests that the distribution of the carbonaceous component of the diffuse ISM is not uniform throughout the Galaxy, but instead may increase in density toward the center of the Galaxy. The similar behavior of the C—H and Si—O stretching bands suggests that these two components may be coupled, perhaps in the form of silicate-core, organic-mantle grains. Several possible models of the distribution of this material are presented and it is demonstrated that the inner parts of the Galaxy has a carrier density that is 5 to 35 times higher than in the local ISM. Depending on the model used, the density of aliphatic material in the local ISM is found to be about 1 to 2 $-CH_3$ groups m^{-3} and about 2 to 5 $-CH_2-$ groups m^{-3}. These densities are consistent with the strengths of the 2955 and 2925 cm^{-1} (3.38 and 3.42 μm) subfeatures (due to $-CH_3$ and $-CH_2-$ groups, respectively) within the overall 2950 cm^{-1} (3.4 μm) band being described by the relations $A_v/\tau_{(2955\ cm^{-1})} = 270 \pm 40$ and $A_v/\tau_{(2925\ cm^{-1})} = 250 \pm 40$ in the *local* diffuse ISM.

Subject headings: infrared: ISM: lines and bands — ISM: molecules

1. INTRODUCTION

The nature of dust in the diffuse interstellar medium (ISM) has recently been the subject of a great deal of study. General parameters such as particle size and shape have been constrained using the UV-visual portion of the excitation curve and polarization measurements. These, in conjunction with cosmic abundance constraints and the optical properties of relevant materials, have been used to place constraints on the dust composition. In general, the dust is believed to consist of mixtures of silicate and carbonaceous materials (see Greenberg & Hong 1974; Mathis, Rumpl, & Nordsieck 1977; Greenberg 1978; Greenberg & Chlewicki 1983; Jones, Duley, & Williams 1987; Mathis & Whiffen 1989). Recent reviews of interstellar dust models, and pertinent references can be found in Greenberg (1989), Mathis (1989), and Williams (1989).

The detection of absorption bands near 3300 and 2950 cm^{-1} (3.0 and 3.4 μm; due to O—H and C—H stretching vibrations, respectively) in the spectra of Galactic center infrared sources (Soifer, Russell, & Merrill 1976; Willner et al. 1979; Wickramasinghe & Allen 1980) led to many follow-up observations and analyses because the features along this line of sight were thought to be due to dust in the diffuse ISM (Allen & Wickramasinghe 1981; Willner & Pipher 1982; Jones, Hyland, & Allen 1983; Wickramasinghe & Allen 1983; Allamandola 1984; Butchart et al. 1986; Tielens & Allamandola 1987; McFadzean et al. 1989). However, these Galactic center studies did not confirm the dust responsible for the features is in the diffuse medium, since the features could have potentially been produced by materials local to the Galactic center itself. Indeed, the work of McFadzean et al. (1989) showed that the broad O—H feature near 3300 cm^{-1} (3.0 μm) varies in strength from source to source in the Galactic center, and they suggested that it is due, at least in part, to local materials. Without additional studies along different lines-of-sight it was difficult to ascertain how much of the 3300 and 2950 cm^{-1} (3.0 and 3.4 μm) absorption bands arise from material local to the Galactic center and how much (if any) arises from the intervening ISM.

Until recently, the only other object toward which the 2950 cm^{-1} (3.4 μm) feature had been detected was VI Cygni 12 (Adamson, Whittet, & Duley 1990). However, recent studies of the 3600–2600 cm^{-1} (2.78–3.85 μm) spectral region of objects along many different lines of sight suffering from a wide range of visual extinctions (A_v), have clarified this issue considerably (Sandford et al. 1991; Pendleton 1994; Pendleton et al. 1994). These papers demonstrated that the 3300 cm^{-1} (3.0 μm) O—H stretching band does not correlate with A_v along different lines-of-sight and therefore is not due primarily to dust in the diffuse ISM, confirming the conclusions of McFadzean et al. (1989). In contrast, the studies of the 2950 cm^{-1} (3.4 μm) C—H stretching band by Sandford et al. (1991) and Pendleton et al. (1994) show there is remarkable similarity in position and profile of this feature over extinctions ranging from as low as 3.9 to as high as 31 (see Fig. 1*a*). In addition, the strength of this feature increases with increasing A_v, suggesting that it *is* largely due to dust in the diffuse ISM.

The profile and subpeak positions of the overall C—H stretching feature provide specific clues to the nature of the carbonaceous material in the diffuse interstellar medium. The hydrocarbon feature extends from about 3000 cm^{-1} (3.33 μm) to 2800 cm^{-1} (3.57 μm) with subfeatures near 2955, 2925, and 2870 cm^{-1} (3.38, 3.42, and 3.48 μm) (Fig. 1). The positions of the first two of these subfeatures are characteristic of the symmetric C—H stretching frequencies of $-CH_3$ (methyl) and $-CH_2-$ (methylene) groups in saturated aliphatic hydrocar-

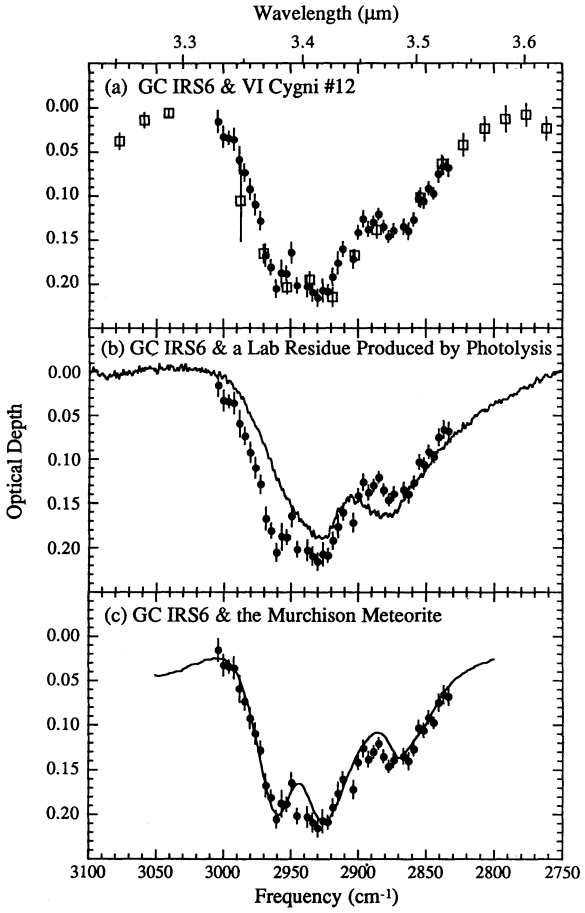

FIG. 1.—Comparison of the optical depth profile of the C—H stretching band due to dust in the diffuse ISM toward GC IRS 6E (A_v = 31 mag; *filled circles*) and: (*a*) VI Cyg 12 (A_v = 10 mag; *open squares*). The VI Cyg 12 data have been scaled to have the same optical depth as the GC IRS 6E data at 2925 cm^{-1}. (*b*) A C-rich laboratory residue produced by the irradiation of an interstellar ice analog (*solid line*) (see Allamandola et al. 1988 for details on the production of the laboratory residue). (*c*) A carbonaceous phase of the Murchison meteorite (*solid line*) [see Pendleton et al. 1994 for further details on the comparisons shown in (*b*) and (*c*)].

bons (molecules with the formula C_nH_{n+2}). The relative strengths of these two subfeatures indicate that the average $-CH_2-/-CH_3$ ratio of the interstellar hydrocarbon is 2.5 ± 0.4. However, the interstellar band profile differs from that of *pure* saturated aliphatic hydrocarbons in that it does not contain the two peaks near 2870 and 2850 cm^{-1} (3.48 and 3.51 μm) characteristic of the asymmetric C—H stretching vibrations of $-CH_3$ and $-CH_2-$ groups, respectively, but instead shows only a single subfeature near 2870 cm^{-1} (3.48 μm). Electronegative or other perturbing chemical groups at the end of short chain aliphatics can suppress the 2850 cm^{-1} (3.51 μm) feature without greatly effecting the positions or strengths of the other three bands. Thus, comparison of laboratory and astronomical data suggests that the 2950 cm^{-1} (3.4 μm) C—H stretch feature produced by dust in the diffuse ISM is largely due to short (n = 2–4) aliphatic chains like $-CH_2-CH_2-CH_3$ and $-CH_2-CH_2-CH_2-CH_3$ attached to electronegative or other perturbing chemical groups like —O—H, —C ≡ N, aromatics, etc. (see Sandford et al. 1991 for a more detailed discussion on the spectral constraints on the diffuse C—H carrier).

Additional constraints on the nature of this material can be provided by spectral comparison with laboratory analogs. In Pendleton et al. (1994), we compared the interstellar feature with the spectra of refractory carbonaceous residues formed by the warming of UV photolyzed interstellar ice analogs (see Fig. 1*b*), hydrogenated amorphous carbon (HAC), quenched carbonaceous composite (QCC), and a carbonaceous fraction of the primitive meteorite Murchison (see Fig. 1*c*). All these materials provided qualitative fits to the interstellar feature, but the match provided by the meteoritic material was clearly best. This suggests that the perturbing chemical groups inferred from the profile of the interstellar feature may consist largely of aromatic moieties since meteoritic kerogen is rich in aromatics. In this regard, the tentative detection by Pendleton et al. (1994) of a weak absorption feature centered near 3030 cm^{-1} (3.3 μm) in the spectra of several Galactic center objects may be especially important. This spectral position is characteristic of the aromatic C—H stretching vibration and suggests that aromatic materials may be present in the diffuse dust in significant concentrations.

In this paper we show that, while the optical depth (τ_{CH}) of the diffuse medium 2950 cm^{-1} (3.4 μm) absorption band increases with increasing A_v, the observed τ_{CH} versus A_v relation indicates that this material is not uniformly distributed throughout the Galaxy. Instead, it appears to be peaked toward the Galactic center.

2. RESULTS AND DISCUSSION

In the following sections we will demonstrate that (1) the carrier of the interstellar C—H stretching feature in the diffuse medium is uniformly distributed in the local ISM but is apparently not uniformly distributed throughout the entire Galaxy (§ 2.1), (2) the overall distribution of the carbonaceous carrier is very similar to that of silicates in the diffuse ISM (§ 2.2), and (3) models that assume an increase in the density of the C—H carrier with decreasing galactic radius can explain the observations (§ 2.3).

2.1. *The τ_{CH}–A_v Relation of Dust in the Diffuse ISM*

Since the profile of the diffuse medium C—H stretching band is relatively constant from object to object, i.e., the subfeatures near 2955, 2925, and 2870 cm^{-1} (3.38, 3.42, and 3.48 μm) have very nearly the same *relative* strengths along all lines of sight (Sandford et al. 1991; Pendleton et al. 1994; Fig. 1*a*), any one of the subfeatures can be used as a tracer of the abundance of the carrier. We will largely restrict the discussion that follows to the 2925 cm^{-1} component since it is the strongest, it is associated with the more abundant $-CH_2-$ groups, and it does not suffer significantly from spectral confusion due to telluric methane.

Table 1 lists the objects for which we know the strength of the interstellar C—H stretching band. Descriptions of these objects and their associated visual extinctions can be found in Sandford et al. (1991), Pendleton et al. (1994), and references therein. With the exception of the objects T629−5 and OH 01−477, which are discussed below, the C—H optical depths and visual extinctions given in Table 1 were taken directly from Sandford et al. (1991) and Pendleton et al. (1994). All the astronomical data used in this paper were obtained at NASA's Infrared Telescope Facility (IRTF).

OH 01−477 and T629−5 are both M stars whose line-of-sight spectra in the 3100–2700 cm^{-1} (3.2–3.7 μm) region are strongly contaminated by photospheric OH absorption lines

TABLE 1

SUMMARY OF OBJECTS CONSIDERED IN THIS STUDY[a]

Object	Object R.A. (1950)	Object Decl. (1950)	Extinction (A_v)	$\tau_{silicate}$[b]	τ_{CH} (2955 cm^{-1})	τ_{CH} (2925 cm^{-1})
GC IRS 7	17^{h}42^{m}29^s.3	−28°59′13″.1	31	3.6 ± 0.4	0.19	0.19
GC IRS 6E.....	17 42 28.9	−28 59 04	31	3.6 ± 0.4	0.205	0.21
GC IRS 3	17 42 29.1	−28 59 14.9	31	3.6 ± 0.4	0.23	0.24
T629−5	18 30 23.0	−08 44 16.6	22		...	0.07[c]
OH 01−477	17 46 12.5	−27 40 49.6	19		...	0.05[c]
AFGL 2179	18 28 56.8	−10 01 23.3	12.8		0.05	0.052
AFGL 2104	18 13 37.0	−18 59 49.0	12.0		0.037	0.044
VI Cygni 12.....	20 30 53.4	+41 03 51.6	10.0	0.58 ± 0.1	0.043	0.046
Ve 2−45	17 59 00.9	−23 37 35.2	6.5		0.02	0.02
BD +40 4220.....	20 30 34.8	+41 08 04	6.2		0.027	0.025
HD 229059.....	20 19 23.0	+37 14 35.0	5.3		0.023	0.028
AS 320.....	18 41 34.0	−03 51 04	5.2	0.26	0.018	0.02
HD 194279.....	20 21 33.0	40 35 48.0	3.9		0.015	0.017

[a] Unless otherwise noted, all values are taken from the best available data in Sandford et al. 1991 and Pendleton et al. 1994. τ_{CH} uncertainties are on the order of 20% and are generally dominated by uncertainties in the baselines underlying the features. A_v-values represent best estimates of the extinction due to the diffuse interstellar material only. All extinctions are in units of magnitudes.

[b] Taken from Roche & Aitken 1985.

[c] Values determined after removal of OH photospheric lines.

which partially obscure the diffuse C—H stretch band toward these objects (Sandford et al. 1991). OH 01−477 is an infrared source whose line of sight is very similar to that of the Galactic center. This object is coincident with an OH source and appears to be a heavily obscured (A_v = 19 mag) M4 III star (Wickramasinghe & Allen 1980; Jones et al. 1982). T269−5 is a very late Mira-type, M8 III star reddened by $A_v \approx 22$ mag (Tapia 1981; Tapia et al. 1989).

The C—H band optical depths given in Table 1 for these two objects were derived by taking the spectra of Sandford et al. (1991) and removing the photospheric OH absorption contribution by subtracting the spectra of unobscured M stars. For unobscured M stars we used ST Ceph and V842 Aql, whose spectra were measured by Pendleton et al. (1994). For several reasons, this process did not result in optical depths or band profiles as precise as those for the other objects listed in Table 1. First, the data for the obscured and unobscured stars were taken during different observing runs and the two sets of data do not agree precisely in resolution and detector positioning. Second, the absolute *and* relative strengths of the OH lines in M star photospheres are quite sensitive to spectral type, so in practice it is difficult to use the spectrum of one M star to exactly cancel the OH lines in the spectrum of another M star. However, none of the stronger OH lines fall near 2925 cm^{-1} (Beer et al. 1972; Sandford et al. 1991; Pendleton et al. 1994) and the derived optical depth of the diffuse C—H stretching absorption feature at this position is relatively insensitive to the interference by photospheric OH. Thus, while it was not possible to perfectly remove the photospheric lines and thereby determine the profile of the C—H stretching features toward T629−5 and OH 01−477, it was possible to use this subtraction technique to obtain reasonable estimates of the optical depths of the 2925 cm^{-1} subfeature toward these objects (Table 1).

Figure 2 shows a plot of A_v versus $\tau_{CH(2925\ cm^{-1})}$ for all the objects in Table 1 (*open and filled circles*). The error bars for the C—H subfeature optical depths are determined from the larger of (1) the statistical error of data points falling in the 2925 cm^{-1} band, or (2) the possible variation of the depth of the 2925 cm^{-1} band optical depth when "extreme" flux baselines were chosen. In this respect, the error bars are conservative, i.e., we show the largest uncertainties. The points near $A_v = 20$ for OH 01−477 and T629−5 have larger than average error bars for the reasons described in the previous paragraph. It is immediately obvious that the strength of the feature increases with increasing A_v, a characteristic that would be expected if the carrier resides in the diffuse ISM.

Sandford et al. (1991) demonstrated that the strength of the 2955 and 2925 cm^{-1} (3.38 and 3.42 μm) subfeatures observed toward the sources they studied could be fit by the relations $A_v/\tau_{(2925\ cm^{-1})} = 310 \pm 90$ and $A_v/\tau_{(2925\ cm^{-1})} = 240 \pm 40$, the largest part of the "uncertainty" arising from the fact that these ratios were significantly different in the Galactic center

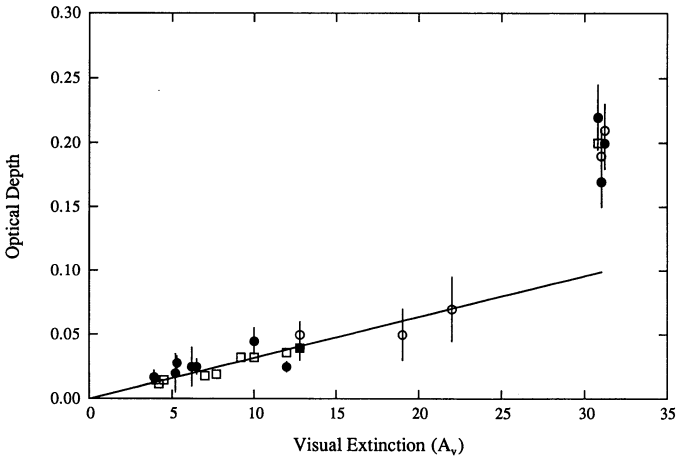

FIG. 2.—Visible extinction (A_v) vs. the optical depth of the C—H and Si—O stretching bands of dust in the diffuse ISM. The filled and open circles are the optical depths of the 2925 cm^{-1} (3.42 μm) —CH_2— band determined from low- and high-resolution data, respectively (Sandford et al. 1991; Pendleton et al. 1994). The open squares are the optical depths of the silicate band near 1000 cm^{-1} (10 μm) (Roche & Aitken 1985). The silicate optical depths have been scaled by a factor of 1/18 to normalize them to the strength of the 2925 cm^{-1} —CH_2— feature at the Galactic Center. (The various points associated with the different sources in the Galactic center have been slightly offset from each other in A_v for clarity).

sources studied. These values were subsequently verified by Pendleton et al. (1994), who studied additional lines of sight, including sources having lower extinctions. They found $A_v/\tau_{(2955\ \mathrm{cm}^{-1})} = 270 \pm 40$ and $A_v/\tau_{(2925\ \mathrm{cm}^{-1})} = 250 \pm 40$ *for the local ISM*. However, it became clear that the band strengths do not increase linearly over the entire A_v range, but instead rise significantly faster at the higher A_v-values associated with the Galactic center sources (see Fig. 2 and Pendleton et al. 1994). The A_v/τ-values for the Galactic center sources alone are $A_v/\tau_{(2925\ \mathrm{cm}^{-1})} = 150 \pm 15$ and $A_v/\tau_{(2925\ \mathrm{cm}^{-1})} = 150 \pm 20$. Thus, the definition of the diffuse C—H subfeature strengths by single A_v/τ ratios, i.e., the assumption of a uniform distribution of the carrier with A_v, may be an over simplification.

At this point it is appropriate to briefly consider whether the anomalous A_v/τ ratios for the Galactic center might be due to an inaccurate estimate of the visual extinction of these objects. For example, if the visual extinction to the Galactic center were actually 60 magnitudes instead of 31 magnitudes, the apparent anomaly would essentially cease to exist. However, there are a number of arguments that suggest that this is not the case. Numerous previous studies have addressed the issue of the visual extinction towards the Galactic center and the published results typically fall in the range of $A_v = 30$–35 magnitudes (see Becklin et al. 1978; Henry, DePoy, & Becklin 1984; Sellgren et al. 1987; Wade et al. 1987; Rieke, Rieke, & Paul 1989). This agreement would seem to be reasonably robust given that these values have been obtained from several different types of objects requiring different assumed intrinsic colors. In addition, using wide field J, H, and K images of the regions surrounding the Galactic center, Glass, Catchpole, & Whitelock (1987) demonstrated that the extinction towards the Galactic center is "patchy" on large spatial scales due to the distribution of foreground interstellar clouds. Examination of the maps shows that all three of our Galactic center sources lie at the edge of one of these clouds in the H and K maps. Glass et al. estimate that the extinction associated with the "edges" of the clouds seen on their H map correspond to extinctions of $A_v \sim 37$ magnitudes. The visibility of the region containing our objects on their H maps is therefore in good agreement with the published values of A_v of 30–35 magnitudes for the Galactic center sources discussed here. Thus, the anomalous A_v/τ ratios associated with the Galactic center appear to be real and the assumption of a uniform distribution of the aliphatic C—H carrier with A_v is not valid. As will be discussed in more detail in § 2.3, a more complicated distribution of material seems to be implied.

2.2. *A Comparison of the Distribution of Carbonaceous Materials and Silicates in the Diffuse ISM*

Included with the τ_{CH}–A_v relation plotted in Figure 2 (*opened and filled circles*) is a similar plot of the depth of the 1000 cm^{-1} (10 μm) Si—O stretching band of silicates in the diffuse ISM (*open squares*). The optical depths for the silicate features were taken from Roche & Aitken (1985), and have been scaled by a factor of 1/18 to match the optical depth of the 2925 cm^{-1} band at the Galactic center. The two sets of data are remarkably similar.

Roche & Aitken (1985) demonstrated that the overall ratio of silicate to visual extinction in the Galactic center is about twice that of the interstellar medium in the solar neighborhood. This implies that the grains responsible for the silicate band are different from those responsible for the observed visual extinction (or at least they are not solely responsible for the visual extinction). It also implies that the dust along the total line of sight to the Galactic center contains a relatively higher proportion of silicates than does the dust in the local solar neighborhood (or, alternatively, the Galactic center contains a lower relative proportion of the material responsible for visual extinction).

The same relative difference between the Galactic center and the local ISM is found for the diffuse C—H stretching band (Fig. 2). This suggests that the silicate and carbonaceous components of the diffuse interstellar medium may be spatially well-correlated and leads to similar conclusions, namely that *the grains responsible for the diffuse medium* C—H *aliphatic stretching band are different from those responsible for much or all of the observed visual extinction and appear to be concentrated toward the Galactic center*. In the following section we will present three simple models that further quantify these points.

2.3. *Models of the Galactic Distribution of Carbonaceous Material in the Diffuse ISM*

It is immediately apparent that a simple line cannot fit all the data in Figure 2. A good linear fit can be made to all the points below $A_v = 22$ mag (solid line in Fig. 2), but the Galactic center points at $A_v = 31$ mag clearly fall well above the extrapolation of this line. As mentioned in the previous section, the nonlinearity of the τ_{CH} versus A_v and $\tau_{silicate}$ versus A_v relations indicate that the carriers responsible for the diffuse medium C—H and Si—O stretching bands are different from those responsible for much of the observed visual extinction. Thus, there are two different, simple means of explaining the τ–A_v relations in Figure 2. These are (1) the source of the observed visual excitation is distributed throughout the Galaxy and the relative abundance of carbonaceous and silicate materials in the diffuse ISM *increases* in the inner parts of the Galaxy, and (2) the carriers of the C—H and Si—O stretching bands are distributed throughout the Galaxy and the relative abundance of the source of the visual extinction *decreases* in the inner parts of the Galaxy. Of course, some combination of these two, or a more complex distribution, is also a possibility. In the interest of simplicity, the discussion that follows will explore the implications that result if case (1) is true, i.e., that the relative abundance of the carriers of the C—H and Si—O stretching bands are larger in the Galactic center. The reader should keep in mind, however, that nothing in our data set preclude the alternative case. We will return briefly to this point later.

Assuming the nonlinearity of the τ–A_v relations in Figure 2 results from an increased relative abundance of the C—H and Si—O carriers toward the Galactic center, several carrier distributions suggest themselves: (1) the distribution of aliphatic carbonaceous materials is more-or-less uniform in the "local" diffuse medium (solar neighborhood) and a smaller volume around the Galactic center contains an unusually high concentration of this material; (2) there is a uniform gradient in the density of aliphatic material in the diffuse medium, with the density increasing linearly toward the Galactic center; or (3) the density distribution of the aliphatic material mimics the stellar mass density distribution, i.e., increases exponentially toward the Galactic center. These possibilities are explored in the following paragraphs using some simple models.

In all the models we assume the density of $-CH_2-$ absorber responsible for the 2925 cm^{-1} band (ρ_{CH_2}) is in units

of $-CH_2-$ groups per cm^2 per unit A_v, and we chose M to be a variable of extinction running over the range $0 < M < 31$ mag. The column density (N_i) of any absorbing species, i, can be determined from

$$N_i = \int \tau_i(\nu_i) d\nu_i / A_i \approx \tau_{\max i} \Delta\nu_{1/2i} / A_i ,$$

where $\int \tau_i(\nu_i) d\nu_i$ is the integrated area of a band associated with the absorber (in cm^{-1}), $\tau_{\max i}$ is the maximum optical depth of the band, $\Delta\nu_{1/2i}$ is the full width at half-maximum (FWHM) of the band (in cm^{-1}), and A_i is the intrinsic strength of that band (in cm molecule^{-1}). Thus, for the specific case of the 2925 cm^{-1} (3.42 μm) interstellar $-CH_2-$ subfeature, we can write

$$\tau_{CH_2} \approx (A_{CH_2}/\Delta\nu_{1/2CH_2}) \int_0^{A_v} \rho_{CH_2}(M) dM , \quad (1)$$

where A_{CH_2} is the integrated absorption strength of the 2925 cm^{-1} subfeature due to C—H stretching vibrations in $-CH_2-$ groups, τ_{CH_2} is the subfeature's maximum optical depth, $\Delta\nu_{1/2CH_2}$ is its full width at half-maximum, and $\rho_{CH_2}(M)$ is the spatial density of the $-CH_2-$ carrier in groups cm^{-2} mag^{-1}.

2.3.1. *Model I—A Uniform $-CH_2-$ Density with a Higher Value near the Galactic Center*

In this model it is assumed that the density (ρ_0) of $-CH_2-$ absorber is constant everywhere in the Galaxy except in a limited region around the Galactic center, where the material is present at a higher density (ρ_{GC}). The crossover to the higher density domain is assumed to occur at an A_v of A_1 where 22 mag $< A_1 <$ 31 mag (see Figs. 2 and 3*a* and Table 2). Thus, we have

$$\rho(M) = \begin{cases} \rho_0 & \text{for } 0 \le M < A_1 \\ \rho_{GC} & \text{for } A_1 \le M < 31 \text{ mag} . \end{cases} \quad (2)$$

Substituting this form of the density into equation (1) yields

$$\tau_{CH_2} = \begin{cases} (A_{CH_2}/\Delta\nu_{1/2CH_2})(\rho_0 A_v) & \text{for 0 mag} \le A_v < A_1 \\ (A_{CH_2}/\Delta\nu_{1/2CH_2})[(\rho_0 A_1) + \rho_{GC}(A_v - A_1)] & \\ \qquad \text{for } A_1 \le A_v < 31 \text{ mag} , \end{cases} \quad (3)$$

which produces an optical depth function (and therefore column density function) of the form shown by the solid line in Figure 3*b*.

It is possible to fit the data in Figure 2 with a function of this form by making a least squares linear fit to all the τ_{CH} data below $A_v = 25$ mag (first segment of solid line in Fig. 3*b*). This fit essentially passes through the T629—5 point at $\tau_{CH_2} = 0.07$

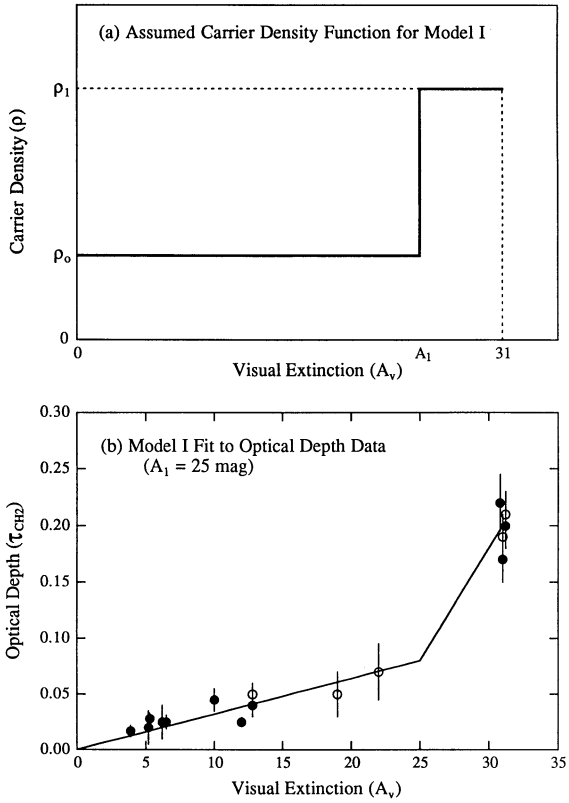

FIG. 3.—(*a*) Density distribution of the carbonaceous carrier assumed in Model I, i.e., the density (ρ_0) of $-CH_2-$ absorber is constant everywhere except in a limited region around the Galactic center, where the material is present at a higher density (ρ_{GC}). (*b*) Comparison between the optical depth function of the 2925 cm^{-1} band and Model I using the parameter values given in Table 2, $A_1 = 25$ mag, and $\rho_{GC} = 0.02$ $-CH_2-$ cm^{-2} mag^{-1} (see text for details). The points have the same meanings as given in Fig. 1.

TABLE 2

SUMMARY OF THE DENSITY MODELS DESCRIBED IN THE TEXT AND THEIR PARAMETERS[a]

Functional Form	Best-Fit Parameters
MODEL I:	
$\tau_{CH_2} = \begin{cases} (A_{CH_2}/\Delta\nu_{1/2CH_2})(\rho_0 A_v) & \text{for } 0 \le A_v < A_1 \\ (A_{CH_2}/\Delta\nu_{1/2CH_2})[(\rho_0 A_1) + \rho_{GC}(A_v - A_1)] & \text{for } A_1 \le A_v < 31 \text{ mag} \end{cases}$	$\rho_0 = 0.0032\ (\Delta\nu_{1/2CH_2}/A_{CH_2})$ mag^{-1} $\rho_{GC} = 0.014$–$0.104\ (\Delta\nu_{1/2CH_2}/A_{CH_2})$ mag^{-1}
$N = \begin{cases} (\rho_0 A_v) & \text{for } 0 \le A_v < A_1 \\ [(\rho_0 A_1) + \rho_{GC}(A_v - A_1)] & \text{for } A_1 \le A_v < 31 \text{ mag} \end{cases}$	22 mag $\le A_1 <$ 31 mag
MODEL II:	
$\tau_{CH_2} = (A_{CH_2}/\Delta\nu_{1/2CH_2})[\rho_0 A_v + \frac{1}{2} C A_v^2]$ $N = [\rho_0 A_v + \frac{1}{2} C A_v^2]$	$\rho_0 = 0.0012\ (\Delta\nu_{1/2CH_2}/A_{CH_2})$ mag^{-1} $C = 0.00032\ (\Delta\nu_{1/2CH_2}/A_{CH_2})$ mag^{-2}
MODEL III:	
$\tau_{CH_2} = (A_{CH_2}/\Delta\nu_{1/2CH_2})[-C_2 + (\rho_0 - C_2)A_v + \frac{1}{2} C_1 A_v^2 + C_2 e A_v]$	$\rho_0 = 0.0027\ (\Delta\nu_{1/2CH_2}/A_{CH_2})$ mag^{-1} $C_1 = 7.16 \times 10^{-5}\ (\Delta\nu_{1/2CH_2}/A_{CH_2})$ mag^{-2}
$N = [-C_2 + (\rho_0 - C_2)A_v + \frac{1}{2} C_1 A_v^2 + C_2 e^{A_v}]$	$C_2 = 2.52 \times 10^{-15}\ (\Delta\nu_{1/2CH_2}/A_{CH_2})$ mag^{-1}

[a] For the diffuse medium 2925 cm^{-1} C—H stretching subfeature due to $-CH_2-$ groups, use $A_{CH_2} = 8 \times 10^{-18}$ cm/CH$_2$ group and $\Delta\nu_{1/2CH_2} = 20$ cm^{-1} (Sandford et al. 1991). All extinctions are in units of magnitudes.

TABLE 3

SUMMARY OF THE CALCULATED LOCAL AND GALACTIC CENTER DENSITIES OF ALIPHATIC $-CH_2-$ IN THE DIFFUSE INTERSTELLAR MEDIUM[a]

Local $-CH_2-$ Density (ρ_0)	Galactic Center $-CH_2-$ Density (ρ_{GC})	(ρ_{GC}/ρ_0)
Model I:		
0.0032 ($\Delta\nu_{1/2CH_2}/A_{CH_2}$) mag^{-1}	0.014 ($\Delta\nu_{1/2CH_2}/A_{CH_2}$) mag^{-1} ($A_1$ = 22 mag) to 0.104 ($\Delta\nu_{1/2CH_2}/A_{CH_2}$) mag^{-1} ($A_1$ = 30 mag)	4.4 (A_1 = 22 mag) to 32.5 (A_1 = 30 mag)
8.0×10^{15} CH_2 cm^{-2} mag^{-1}	3.5×10^{16} CH_2 cm^{-2} mag^{-1} (A_1 = 22 mag) to 2.6×10^{17} CH_2 cm^{-2} mag^{-1} (A_1 = 30 mag)	4.4 (A_1 = 22 mag) to 32.5 (A_1 = 30 mag)
5.2×10^{-6} CH_2 cm^{-3} = 5.2 CH_2 m^{-3}	2.3×10^{-5} CH_2 cm^{-3} (A_1 = 22 mag) to 1.7×10^{-4} CH_2 cm^{-3} (A_1 = 30 mag) = 23–170 CH_2 m^{-3}	4.4 (A_1 = 22 mag) to 32.5 (A_1 = 30 mag)
Model II:		
0.0012 ($\Delta\nu_{1/2CH_2}/A_{CH_2}$) mag^{-1}	0.011 ($\Delta\nu_{1/2CH_2}/A_{CH_2}$) mag^{-1}	9.2
3.0×10^{15} CH_2 cm^{-2} mag^{-1}	2.8×10^{16} CH_2 cm^{-2} mag^{-1}	9.2
2.0×10^{-6} CH_2 cm^{-3} = 2.0 CH_2 m^{-3}	1.8×10^{-4} CH_2 cm^{-3} = 18 CH_2 m^{-3}	9.2
Model III:		
0.0027 ($\Delta\nu_{1/2CH_2}/A_{CH_2}$) mag^{-1}	0.078 ($\Delta\nu_{1/2CH_2}/A_{CH_2}$) mag^{-1}	28.6
6.9×10^{15} CH_2 cm^{-2} mag^{-1}	2.0×10^{17} CH_2 cm^{-2} mag^{-1}	28.6
4.4×10^{-6} CH_2 cm^{-3} = 4.4 CH_2 cm^{-3}	1.3×10^{-4} CH_2 cm^{-3} = 130 CH_2 cm^{-3}	28.6

[a] For the diffuse medium 2925 cm^{-1} C—H stretching subfeature due to $-CH_2-$ groups, use $A_{CH_2} = 8 \times 10^{-18}$ cm/CH_2 group and $\Delta\nu_{1/2CH_2} = 20$ cm^{-1} (Sandford et al. 1991). All extinctions are in units of magnitudes.

and $A_v = 22$ mag. Substituting these values into the top half of equation (2) yields $\rho_0 = 0.0032\ (\Delta\nu_{1/2CH_2}/A_{CH_2})$ mag^{-1}. For the 2925 cm^{-1} $-CH_2-$ band, $\Delta\nu_{1/2CH_2} \approx 20$ cm^{-1} and $A_{CH_2} \approx 8 \times 10^{-18}$ cm/CH_2 group (Sandford et al. 1991). Assuming an average extinction-to-distance ratio of 2 magnitudes per kpc (Allen 1976), this corresponds to a local density of ~ 5 $-CH_2-$ groups m^{-3} (Table 3) and is consistent with a local value of $A_v/\tau_{(2925\ cm^{-1})} = 250$. The local diffuse medium density of H is $\sim 10^5$ H atoms m^{-3} (Allen 1976). Since the $-CH_2-/-CH_3$ ratio of the diffuse medium carrier is 2.0–2.5 (Sandford et al. 1991) this corresponds to a local density of ~ 2 to 3 $-CH_3$ groups m^{-3}.

Using equation (3) and the derived value for ρ_0, one can place limits on the density of aliphatic material implied for the Galactic center, where $\tau_{CH_2} = 0.2$ and $A_v = 31$ mag. In this case we can only derive limits since we do not know the appropriate value of A_1. However, A_1 must lie above $A_v = 22$ mag and below $A_v = 31$ mag (Fig. 2). Substituting the appropriate values into the lower half of equation (2) yields a lower density limit (corresponding to $A_1 \approx 22$ mag) of $\rho_{GC} = 0.014\ (\Delta\nu_{1/2CH_2}/A_{CH_2})$ mag^{-1} an and upper limit (corresponding to $A_1 \approx 30$ mag) of $\rho_{GC} = 0.104\ (\Delta\nu_{1/2CH_2}/A_{CH_2})$ mag^{-1}. Using the same values of $\Delta\nu_{1/2CH_2}$, A_{CH_2}, and extinction-to-distance ratio given above, this corresponds to a range in Galactic center densities of about 25 to 170 $-CH_2-$ groups m^{-3} (Table 3). Thus, Model I requires the density of diffuse medium aliphatic materials ($-CH_2-$ and $-CH_3$ groups) to be a factor of ~ 5 to 35 times higher in the Galactic center than it is locally, depending on the value of A_1.

2.3.2. *Model II—A $-CH_2-$ Density that Increases Linearly toward the Galactic Center*

In Model II it is assumed that the local density of $-CH_2-$ absorber is ρ_0 and that the density increases linearly as one approaches the Galactic center (Fig. 4*a*). Thus, we have

$$\rho(M) = \rho_0 + CM \quad \text{for } 0 \le M < 31 \text{ mag}, \tag{4}$$

where C is a constant. Substituting this form of the density into equation (1) yields

$$\tau_{CH_2} = (A_{CH_2}/\Delta\nu_{1/2CH_2})[\rho_0 A_v + \tfrac{1}{2}CA_v^2], \tag{5}$$

which produces an optical depth function (and therefore column density function) of the form shown as a solid line in Figure 4*b*.

The best-fit curve to the data points in Figure 2 having the functional form of equation (5) and constrained to pass through the origin is $\tau_{CH_2} = 0.0012A_v + 0.00016A_v^2$ (solid line in Fig. 4*b*, Table 2). Equating the first-order terms yields a local space density of $-CH_2-$ groups of $\rho_0 = 0.0012\ (\Delta\nu_{1/2CH_2}/A_{CH_2})$ mag^{-1}. This is a factor of ~ 3 lower than the local density derived using Model I. Using the same values of $\Delta\nu_{1/2CH_2}$, A_{CH_2}, and extinction-to-distance ratio used in Model I, this corresponds to a local density of ~ 2 $-CH_2-$ groups m^{-3} (Table 3) and about 1 $-CH_3$ group m^{-3}.

Equating the second order terms of equation (5) and the best fit to the data yields $C = 0.00032\ (\Delta\nu_{1/2CH_2}/A_{CH_2})$ mag^{-2}. Substituting the appropriate values for ρ_0 and C into equation (4) and using $A_v = 31$ mag yields a calculated Galactic center density of $\rho_{GC} = 0.011\ (\Delta\nu_{1/2CH_2}/A_{CH_2})$ mag^{-1}. This is a factor

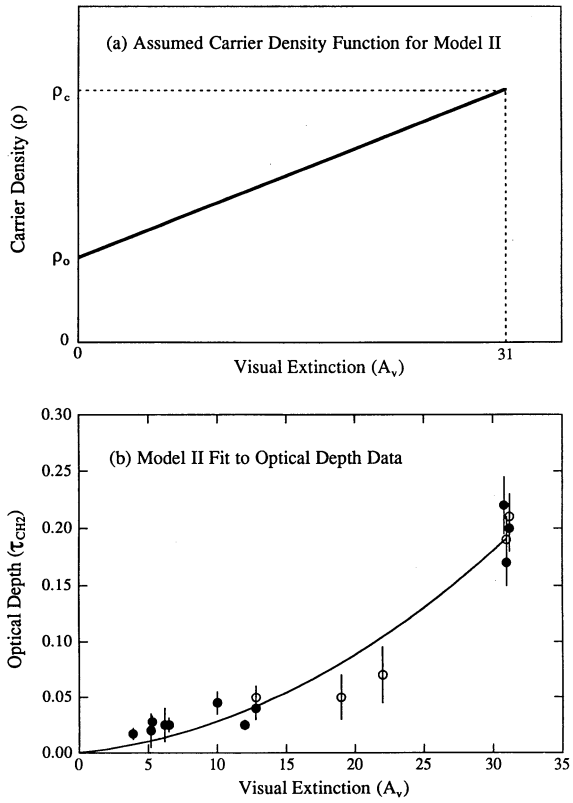

FIG. 4.—(*a*) Density distribution of the carbonaceous carrier assumed in Model II, i.e., the local density of $-CH_2-$ absorber is ρ_0 and the density increases linearly toward the Galactic center. (*b*) Comparison between the optical depth function of the 2925 cm^{-1} band and Model II using the parameter values given in Table 2 (see text for details). The points have the same meanings as given in Fig. 1.

of 1.3 to 9.5 times smaller than that derived using Model I. Using the usual values of $\Delta\nu_{1/2CH_2}$, A_{CH_2}, and extinction-to-distance ratio, this corresponds to a Galactic center density of ~ 20 $-CH_2-$ groups m^{-3} (Table 3) and ~ 10 $-CH_3$ groups m^{-3}. Thus, Model II requires the density of diffuse medium aliphatic materials to be a factor of ~ 10 times higher in the Galactic center than it is in the local diffuse ISM.

2.3.3. *Model III—A* $-CH_2-$ *Density that Increases Exponentially toward the Galactic Center*

In Model III it is assumed that the density of $-CH_2-$ increases exponentially as one approaches the Galactic center and has a local density of ρ_0 (Fig. 5*a*), i.e.,

$$\rho(M) = (\rho_0 - C_2) + C_1 M + C_2 e^M \quad \text{for } 0 \le M < 31 \text{ mag}, \tag{6}$$

where C_1 and C_2 are constants. This distribution mimics the form of the stellar density function in the galactic plane (see Allen 1976, p. 285, and references therein). Substituting the above form of the density into equation (1) yields

$$\tau_{CH_2} = (A_{CH_2}/\Delta\nu_{1/2CH_2})[-C_2 + (\rho_0 - C_2)A_v + \tfrac{1}{2}C_1 A_v^2 + C_2 e^{A_v}], \tag{7}$$

which produces an optical depth function (and therefore column density function) of the form shown as a solid line in Figure 5*b*.

The best-fit curve to the data points in Figure 2 having the functional form of equation (7) is $\tau_{CH_2} = -2.52 \times 10^{-15} + 2.74 \times 10^{-3} A_v + 3.58 \times 10^{-5} A_v^2 + 2.52 \times 10^{-15} e^{A_v}$ (solid line in Fig. 5*b*, Table 2). Equating the zeroth- and second-order terms of this expression with the same terms in equation (7) yields $C_1 = 7.16 \times 10^{-5}$ $(\Delta\nu_{1/2CH_2}/A_{CH_2})$ mag^{-2} and $C_2 = 2.52 \times 10^{-15}$ $(\Delta\nu_{1/2CH_2}/A_{CH_2})$ mag^{-1}. Equating the first order terms and using the derived value of C_2, we find a local $-CH_2-$ group density of $\rho_0 = 0.0027$ $(\Delta\nu_{1/2CH_2}/A_{CH_2})$ mag^{-1}. This is similar to the local density derived using Model I and ~ 2 times higher than in Model II. Using the same values of $\Delta\nu_{1/2CH_2}$, A_{CH_2}, and extinction-to-distance ratio used in Model I, this corresponds to a local density of ~ 4–5 $-CH_2-$ groups m^{-3} (Table 3) and about 2 $-CH_3$ group m^{-3}.

Substituting the appropriate values for ρ_0, C_1, and C_2 into equation (6) and using $A_v = 31$ mag yields a calculated Galactic center density of $\rho_{GC} = 0.078$ $(\Delta\nu_{1/2CH_2}/A_{CH_2})$ mag^{-1}. This is a factor of 7 times larger than that derived using Model II and falls in the upper part of the range derived using Model I. Using the usual values of $\Delta\nu_{1/2CH_2}$, A_{CH_2}, and extinction-to-distance ratio, this corresponds to a Galactic center density of ~ 130 $-CH_2-$ groups m^{-3} (Table 3) and ~ 70 $-CH_3$ groups m^{-3}. Thus, Model III requires the density of diffuse medium aliphatic materials to be a factor of ~ 30 times higher in the Galactic center than it is in the local diffuse ISM.

2.3.4. *Implications of the Model* $-CH_2-$ *Density Distributions*

The parameters of Models I, II, and III, along with their predicted local and Galactic center diffuse medium $-CH_2-$ densities, are summarized in Tables 2 and 3. All three models

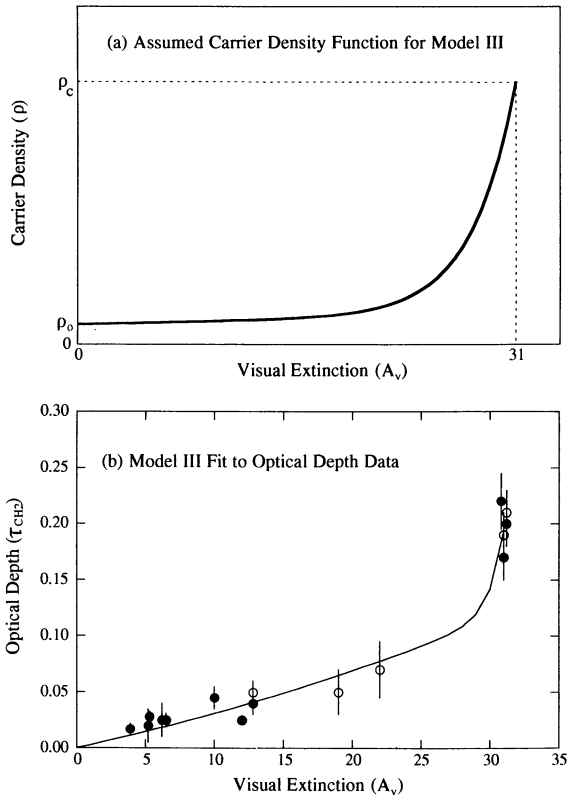

FIG. 5.—(*a*) Density distribution of the carbonaceous carrier assumed in Model III, i.e., the local density of $-CH_2-$ absorber is ρ_0 and the density increases exponentially as one approaches the Galactic center. (*b*) Comparison between the optical depth function of the 2925 cm^{-1} band and Model III using the parameter values given in Table 2 (see text for details). The points have the same meanings as given in Fig. 1.

indicate that the density of the diffuse medium aliphatic carrier is higher in the inner Galaxy than it is in the solar neighborhood. The extent to which the density in the inner Galaxy is higher is model dependent, but it appears that it must be higher by *at least* a factor of 5. Galactic center density enhancements by factors as large as 35 are required if the local density is typical of most of the Galaxy.

It is presently difficult to choose between these carrier distributions because of the paucity of good data at extinctions between 20 and 30 magnitudes, the range that discriminates most strongly between the models. Models I and III seem to produce better fits to the data than Model II, but this statement is based largely on the better fit to the two least certain points near $A_v = 20$ mag. Clearly, additional data in the 20 to 30 magnitude extinction range would be useful for further constraining the spatial distribution of this carbonaceous carrier in the diffuse ISM.

At this point it is appropriate to remind the reader of several points. First, while the previous discussion was addressed specifically to the distribution of the carbonaceous material in the diffuse ISM, the close match shown in Figure 2 to the diffuse silicate distribution determined by Roche & Aitken (1985) indicates that the same general conclusions apply to this material as well, i.e., silicates in the diffuse medium would be similarly concentrated in the inner portions of the Galaxy and by similar factors. Second, we remind the reader that the above discussion was based on the assumption that the nonlinearity of the C—H and Si—O stretching band $\tau - A_v$ relationships is due to relative abundance enhancements of their carriers with respect to the distribution of the source(s) of visual extinction toward the center of the Galaxy. Presumably, one could also explain Figure 2 by assuming that the C—H and Si—O band carriers are distributed throughout the Galaxy and there is an under-abundance of nonaliphatic, nonsilicate, extinction-producing material in the central regions of the Galaxy. In this case, the implied abundance gradients would have similar magnitudes to those discussed above, but they would be reversed in sense and would apply to the material responsible for the visual extinction, not the C—H and Si—O carrier materials.

2.4. *Potential Causes of the Nonuniform Distribution of the Diffuse ISM Aliphatic* C—H *Carrier*

The origin of the nonuniformity in the distribution of the diffuse medium carriers of the aliphatic C—H and silicate Si—O stretching bands with respect to visual extinction is not clear. If the actual distribution of the carrier is similar to the step function used in Model I, the discontinuity at $A_v = A_1$ (Fig. 3*a*) might be associated with the transition from the ISM in the galactic disk to the central bulge. Alternatively, it might be associated with some more localized structure associated with the center of the Galaxy, for example, the circumnuclear molecular disk known to surround the Galactic center (see Kundt 1990 for a review).

The nonuniformity of the C—H and Si—O carriers may be the result of metallicity gradients within the Galaxy. Observations of H II regions and supernovae remnants (SNR) in other spiral galaxies show that an increase in the O/H, N/H, and S/H ratios of about 3 to 5 is not uncommon between the outskirts and centers of such galaxies (see Dopita, D'Odorico, & Benvenuti 1980; Blair, Kirshner, & Chevalier 1982; Blair & Kirchner 1985). Observations of H II regions and SNR within our own Galaxy indicate similar gradients for O/H, N/H, and C/H (see Binette et al. 1982; Shaver et al. 1983; Fesen, Blair, & Kirshner 1985; Meyer 1989). Such gradients appear to be a natural result of galactic chemical evolution (see Matteucci & Francois 1989; Matteucci 1991; Rana 1991, and references therein).

Thus, the increased spatial density of the carbonaceous carrier of the aliphatic C—H band toward the Galactic center might be the result of an increased relative abundance of available carbon. If this were the case, then one would expect the behavior of the τ_{CH}–A_v relation to mimic, to some extent, metallicity. In this regards, it is interesting to note that recent studies of the abundance gradients of N, O, Ne, and S in our Galaxy not only confirm that metallicity increases toward the Galactic center, but suggest the possibility that the increases may occur in discrete steps rather than continuously (Simpson et al. 1995). Such a noncontinuous distribution is consistent with the fit provided to our τ_{CH}–A_v relation by Model I.

Unfortunately, this explanation produces a new dilemma, namely, it requires that the materials responsible for the visual extinction do not track metallicity, or at least not in the same way as do the carriers of the C—H and Si—O bands. Given that the material responsible for the visual extinction must also contain an abundance of elements heavier than H and He, this comes as a surprise. Perhaps both types of material track metallicity, but the carriers of the C—H and Si—O bands increase with metallicity at a much greater rate.

Finally, in their studies of the Si—O stretching feature of silicates in the diffuse ISM, Roche & Aitken (1985) assumed that the nonlinearity of their τ_{SiO}–A_v relation was due to the depletion of carbon stars in the central regions of the Galaxy, noting that models like that of Mathis et al. (1977) predict that most of the visible extinction comes from grains in carbon-rich environments. This type of scenario was mentioned briefly earlier and is the compliment of the models discussed here, i.e., it corresponds to a model in which the carriers of the C—H and Si—O stretching bands are more-or-less uniformly distributed in the Galaxy and the relative abundance of the source of the extra visual extinction *decreases* in the inner parts of the Galaxy. As mentioned previously, there is nothing in the current τ-A_v data that precludes this possibility. *However, this interpretation is only consistent with our findings if the carbonaceous material produced by carbon stars is different from the carbonaceous material responsible for the* 2950 cm^{-1} *band*, i.e. the C—H band carrier is not made by carbon stars and the material made by these stars produces significant visual extinction. We note that this possibility is consistent with the interpretation that the carrier of the diffuse ISM C—H stretching band is due to refractory organics produced in dense clouds by the irradiation of ice mantles (Sandford et al. 1991), not in carbon stars, and offers a natural explanation of the similarities in the τ_{SiO}–A_v and τ_{CH}–A_v relations since the silicate grains may constitute a large fraction of the core grains on which the ices are condensed. In this regard, our findings are consistent with the kinds of core-mantle grains suggested by Greenberg and discussed in Greenberg (1978) and Hong & Greenberg (1980).

3. CONCLUSIONS

The infrared feature in absorption near 2950 cm^{-1} (3.4 μm) in the spectra of many stars suffering from interstellar extinction is attributed to aliphatic C—H stretching vibrations in carbonaceous dust in the diffuse interstellar medium (ISM). The strength of the diffuse C—H stretching band (τ_{CH}) does not scale linearly with visual extinction (A_v) throughout the Galaxy, but instead increases more rapidly in the vicinity of the

Galactic center. This implies that the grains responsible for the diffuse medium C—H aliphatic stretching band are different from those responsible for much of the observed visual extinction. This also suggests that the distribution of the carbonaceous component of the diffuse ISM is not uniform throughout the Galaxy.

Several simple models of the distribution of the material were presented. It was demonstrated that, while the inferred increase in carrier density towards the Galactic center is model dependent, the inner part of the Galaxy has a relative carrier density that is at least 5 times higher than the local ISM and which could be as much as 35 times higher. Depending on the model used, the local space density of $-CH_2-$ groups in the carrier can range from about 2 to 5 $-CH_2-$ groups m^{-3}. The density of $-CH_3$ groups in this material are a factor of 2.0 to 2.5 times smaller. These densities are consistent with the strengths of the 2955 and 2925 cm^{-1} subfeatures (due to $-CH_3$ and $-CH_2-$ groups, respectively) being described by the relations $A_v/\tau_{(2955\ cm^{-1})} = 270 \pm 40$ and $A_v/\tau_{(2925\ cm^{-1})} = 250 \pm 40$ in the local diffuse ISM. Additional high quality measurements, especially of objects suffering extinctions in the $A_v = 20$–30 mag range, will be needed to better constrain the carrier density distribution.

The relationship between the strength of the 2950 cm^{-1} (3.4 μm) diffuse band (τ_{CH}) and visual extinction (A_v) closely matches that of silicate materials in the diffuse ISM, suggesting that the silicate and organic components of the diffuse interstellar medium are spatially well-correlated. In this regard, our findings are consistent with the idea that the silicates and the carbonaceous material responsible for the 2950 cm^{-1} band are in the form of core-mantle grains. The close correlation of the strengths of the silicate Si—O and aliphatic C—H stretching bands and their simultaneous lack of linear correlation with A_v indicates that a substantial portion of the visual extinction in the diffuse interstellar medium is produced by an additional, spatially uncorrelated component or components.

We are grateful to M. Bernstein, M. Haas, J. Simpson, and especially T. Roellig for useful discussions. The paper also benefitted for the remarks of an anonymous referee. This work was supported in part by NASA grants 199-52-12-04 and 185-52-12-09 (Exobiology), 452-33-93-03 (Origins of Solar Systems), and 188-44-21-04 (Astrophysics).

REFERENCES

Adamson, A. J., Whittet, D. C. B., & Duley, W. W. 1990, MNRAS, 243, 400
Allamandola, L. J. 1984, in Galactic and Extragalactic Infrared Spectroscopy, ed. M. Kessler & P. Phillips (Dordrecht: Reidel), 5
Allamandola, L. J., Sandford, S. A., & Valero, G. J. 1988, Icarus, 76, 225
Allen, C. W. 1976, Astrophysical Quantities (London: Athlone)
Allen, D. A., & Wickramasinghe, D. T. 1981, Nature, 294, 239
Becklin, E. E., Matthews, K., Neugebauer, G., & Willner, S. P. 1978, ApJ, 220, 831
Beer, R., Hutchison, R. B., Norton, R. H., & Lambert, D. L. 1972, ApJ, 172, 89
Binette, L., Dopita, M. A., D'Odorico, S., & Benvenuti, P. 1982, A&A, 115, 315
Blair, W. P., & Kirshner, R. P. 1985, ApJ, 289, 582
Blair, W. P., Kirshner, R. P., & Chevalier, R. A. 1982, ApJ, 254, 50
Butchart, I., McFadzean, A. D., Whittet, D. C. B., Geballe, T. R., & Greenberg, J. M. 1986, A&A, 154, L5
Dopita, M. A., D'Odorico, S., & Benvenuti, P. 1980, ApJ, 236, 628
Fesen, R. A., Blair, W. P., & Kirshner, R. P. 1985, ApJ, 292, 29
Glass, I. S., Catchpole, R. M., & Whitelock, P. A. 1987, MNRAS, 227, 373
Greenberg, J. M. 1978, in Cosmic Dust, ed. J. A. M. McDonnell (New York: Wiley), 187
———. 1989, in Interstellar Dust, ed. L. J. Allamandola & A. G. G. M. Tielens (Dordrecht: Kluwer), 345
Greenberg, J. M., & Chlewicki, G. 1983, ApJ, 272, 563
Greenberg, J. M., & Hong, S. S. 1974, in ESLAB Symp. 8, ed. A. F. M. Moorwood (ESRO SP-105), 153
Henry, J. P., DePoy, D. L., & Becklin, E. E. 1984, ApJ, 285, L27
Hong, S., & Greenberg, J. M. 1980, A&A, 88, 194
Jones, A. P., Duley, W. W., & Williams, D. A. 1987, MNRAS, 229, 213
Jones, T. J., Hyland, A. R., & Allen, D. A. 1983, MNRAS, 205, 187
Jones, T. J., Hyland, A. R., Caswell, J. L., & Gatley, I. 1982, ApJ, 253, 208
Kundt, W. 1990, A&SS, 172, 109
Mathis, J. S. 1989, in Interstellar Dust, ed. L. J. Allamandola & A. G. G. M. Tielens (Dordrecht: Kluwer), 357
Mathis, J. S., Rumpl, W., & Nordsieck, K. H. 1977, ApJ, 217, 425
Mathis, J. S., & Whiffen, G. 1989, ApJ, 341, 808
Matteucci, F. 1991, in ASP Conf. Ser. 20, Frontiers of Stellar Evolution, ed. D. L. Lambert (San Francisco: ASP), 539
Matteucci, F., & Francois, P. 1989, MNRAS, 239, 885
McFadzean, A. D., Whittet, D. C. B., Longmore, A. J., Bode, M. F., & Adamson, A. J. 1989, MNRAS, 241, 873
Meyer, J.-P. 1989, in Cosmic Abundances of Matter, ed. C. J. Waddington (New York: AIP), 245
Pendleton, Y. 1994, in ASP Conf. Ser. 58, Infrared Cirrus and Diffuse Dust, ed. R. Cutri & W. Latter (San Francisco: ASP), in press
Pendleton, Y. J., Sandford, S. A., Allamandola, L. J., Tielens, A. G. G. M., & Sellgren, K. 1994, ApJ, 437, 683
Rana, N. C. 1991, ARA&A, 29, 129
Rieke, G. H., Rieke, M. J., & Paul, A. E. 1989, ApJ, 336, 752
Roche, P. F., & Aitken, D. K. 1985, MNRAS, 215, 425
Sandford, S. A., Allamandola, L. J., Tielens, A. G. G. M., Sellgren, K., Tapia, M., & Pendleton, Y. 1991, ApJ, 371, 607
Sellgren, K., Hall, D. N. B., Kleinmann, S. G., & Scoville, N. Z. 1987, ApJ, 317, 881
Shaver, P. A., McGee, R. X., Newton, L. M., Danks, A. C., & Pottasch, S. R. 1983, MNRAS, 204, 53
Simpson, J. P., Colgan, S. W. J., Rubin, R. H., Erickson, E. F., & Haas, M. R. 1995, ApJ, 444, in press
Soifer, B. T., Russell, R. W., & Merrill, R. M. 1976, ApJ, 207, L83
Tapia, M. 1981, MNRAS, 197, 949
Tapia, M., Persi, P., Roth, M., & Ferrari-Toniolo, M. 1989, A&A, 225, 488
Tielens, A. G. G. M., & Allamandola, L. J. 1987, in Physical Processes in Interstellar Clouds, ed. G. E. Morfill, & M. Scholer (Dordrecht: Reidel), 333
Wade, R., Geballe, T. R., Krisciunas, K., Gatley, I., & Bird, M. C. 1987, ApJ, 320, 570
Wickramasinghe, D. T., & Allen, D. A. 1980, Nature, 287, 518
———. 1983, A&SS, 97, 369
Williams, D. 1989, in Interstellar Dust, ed. L. J. Allamandola & A. G. G. M. Tielens (Dordrecht: Kluwer), 367
Willner, S. P., & Pipher, J. L. 1982, in AIP Conf. Proc. No. 83, The Galactic Center, ed. G. R. Reigler & R. D. Blandford (New York: AIP), 77
Willner, S. P., Russell, R. W., Puetter, R. C., Soifer, B. T., & Harvey, P. M. 1979, ApJ, 229, L65